



Isoform-selective inhibition of chrysin towards human cytochrome P450 1A2. Kinetics analysis, molecular docking, and molecular dynamics simulations

Lin He^{a,†}, Fan He^{a,b,†}, Huichang Bi^a, Jiankang Li^a, Su Zeng^c, Hai-Bin Luo^{a,*}, Min Huang^a

^a School of Pharmaceutical Sciences, Sun Yat-Sen University, Guangzhou 510006, China

^b Guangzhou Women and Children's Medical Center, Guangzhou 510520, China

^c College of Pharmaceutical Sciences, Zhejiang University, Hangzhou 310058, China

ARTICLE INFO

Article history:

Received 8 June 2010

Revised 24 July 2010

Accepted 16 August 2010

Available online 20 August 2010

Keywords:

Chrysin

1A2

2C9

Selectivity

MD simulations

Kinetics analysis

ABSTRACT

Our kinetics studies demonstrated that the nature product chrysin exhibited a high inhibitory affinity of 54 nM towards human cytochrome P450 1A2 and was comparable to α -naphthoflavone (49 nM), whereas it represented a moderate affinity of 5225 nM against human cytochrome P450 2C9. However, it remains unclear how this inhibitor selectively binds 1A2. To better understand the isoform selectivity of chrysin, molecular docking and molecular dynamics simulations were performed. Chrysin formed a strong H-bond with Asp313 of 1A2. The stacking interactions with Phe226 also contributed to its tight binding to 1A2. The larger and much more open active site architectures of 2C9 may explain the weaker inhibitory affinity of chrysin towards 2C9. The predicted binding free energies suggest that chrysin preferred 1A2 ($\Delta G_{\text{bind, pred}} = -23.11$ kcal/mol) to 2C9 (-20.41 kcal/mol). Additionally, the present work revealed that 7-hydroxy-flavone bound to 1A2 in a similar pattern as chrysin and represented a slightly less negative predicted binding free energy, which was further validated by our kinetics analysis ($IC_{50} = 240$ nM). Results of the study can provide insight for designing novel isoform-selective 1A2 inhibitors.

© 2010 Elsevier Ltd. All rights reserved.

Human cytochrome P450 1A2 belongs to a subfamily of heme-containing proteins involved in the metabolism of numerous ingested foreign compounds (e.g., drugs, carcinogens, food, and pollutants).¹ 1A2 is expressed principally in hepatic tissues, and constitutes approximately 13% of the total cytochrome P450 content. About 5–10% of the clinical drugs are metabolized by 1A2.¹ 1A2 has also been identified as one of the most important enzymes responsible for the activation of precarcinogens, including aromatic and heterocyclic amines and polycyclic aromatic hydrocarbons.^{2–4} Additionally, 1A2's metabolic activity has a close relationship with the human cancer.^{5,6} Hence, a better understanding of the inhibitory mechanisms towards 1A2 has special significance, which contributes to new methods and directions in preventing and curing human cancers caused by environmental chemical carcinogens. A number of studies have revealed that flavonoids exhibit a protective effect on various types of cancer.^{7–10} The mechanisms responsible for the effects are related to flavonoid's inhibition against 1A2. For example, furafylline and α -naphthoflavone (ANF) are known as 1A2's potent inhibitors and help to prevent 1A2-mediated chemical carcinogenesis.^{11–13}

* Corresponding author. Tel.: +86 20 39943031.

E-mail address: luohb77@mail.sysu.edu.cn (H.-B. Luo).

[†] These authors contribute equally.

Chrysin (5,7-dihydroxy-flavone) is a natural, biologically active flavonoid compound extracted from many plants, honey, and propolis. In the present study, chrysin experimentally exhibited a strong inhibitory affinity of 54 nM towards 1A2 and was comparable to ANF (49 nM), which was determined by our previously developed in vitro 'cocktail' method,¹⁴ whereas it represented a moderate affinity of 5225 nM against its isoform cytochrome P450 2C9. However, it remains unknown how chrysin selectively binds 1A2. Based on the recently resolved structure for 1A2 with bound ANF,¹⁵ molecular docking, molecular dynamics (MD) simulations, and MM-PBSA (Molecular Mechanics Poisson–Boltzmann Surface Area) binding free energy calculations were performed to obtain a complete picture of the structural characteristics of chrysin within the active sites of 1A2/2C9, and to better understand the inhibitory mechanism of chrysin. In addition, comparative kinetics analysis on 7-hydroxy-flavone was carried out to qualitatively validate their inhibitory effect as predicted by the binding energy calculations. Reported here are the kinetics of chrysin against 1A2/2C9 and its simulation models to provide insight into the isoform selectivity of 1A2 inhibitors.

Chrysin and 7-hydroxy-flavone (>99% purity) were kindly provided by Professor Zhong Zuo (School of Pharmacy, The Chinese University of Hong Kong). ANF (>99% purity) was purchased from Sigma. NADPH tetrasodium salt was purchased from AppliChem, German. HPLC-grade methanol and formic acid were purchased

from Tedia Company Inc. (Fairfield, OH, USA). All other reagents were of analytical grade. Ultra-pure water was obtained from a Milli-Q Plus water purification system (Millipore, Bedford, MA, USA). Human livers, used to prepare the microsomes in the present study, were obtained from the First Affiliated Hospital of Sun Yat-Sen University as a surplus from liver transplantation donors. The collection of surplus tissue was approved by the Ethics Committee of the Medical Faculty of Sun Yat-Sen University, China. The livers were transferred to ice immediately after the surgical excision, cut into pieces, and stored at -80°C until the microsomes were prepared. Only tumor-free tissue was used for the experiments. The Surveyor HPLC system consisted of a solvent pump and an auto-sampler (Finnigan, San Jose, CA, USA). The separation was achieved using a commercially available Waters Xterra MS C_{18} ($100 \times 2.1 \text{ mm}$, $5 \mu\text{m}$) column. A Finnigan TSQ Quantum triple-quadrupole mass spectrometer equipped with an ESI source was used for mass analysis and detection.

The experimental assays to investigate the inhibitory potential of flavonoids against 1A2/2C9/2D6/3A4 were based on in vitro 'cocktail' approach, which was developed by our lab as a robust, rapid, and sensitive LC/MS/MS method for the determination of the inhibitory affinities of chemicals on CYP enzymes.¹⁴ Four CYP isoforms (1A2, 2C9, 2D6, and 3A4) was used for the current study. All other conditions (including incubations, sample analysis, and calculations) and methods were the same as our recently published article.¹⁴ The IC_{50} values were measured from triplicate determinations with the relative standard deviation error of below 3%.

The X-ray structures of the human microsomal P450 1A2 with bound ANF¹⁵ and 2C9 with bound S-warfarin (SWF)¹⁶ were taken from the PDB (code: 2HI4 and 1OG5), respectively. The N-terminal transmembrane helices were truncated in all structures. Hydrogen atoms were added to the two systems. All ionizable residues were set at their default protonation states at a neutral pH.

The CDOCKER protocol implemented in Accelrys Discovery Studio 2.1¹⁷ was used for the docking procedure. The ligand-binding site of 1A2 was constructed by using ANF as a reference ligand. ANF and chrysin were docked into the input site sphere, defined with a radius of 10 \AA from the center of the ligand-binding site. A conformational search of each ligand was performed using a simulated annealing molecular dynamics approach. The ligands were heated to a temperature of 700 K in 2000 steps and then annealed to 300 K in 5000 steps. The grid extension was set to 8 \AA . Ten random conformations were generated for each ligand. A final minimization step was applied to each ligand docking poses. Residues which located inside the 10 \AA interaction sphere were allowed to move during minimization. The rest of the parameters were set to the default values. From the top 10 poses with relatively lower docking score, we choose the optimal one based on both the docking energy and cluster popularity for further molecular simulation studies. Cluster analysis was carried out on the docking results to decide the best receptor-ligand-binding mode using a root mean square (RMS) tolerance of 1.0 \AA . The same docking protocols were applied to all the ligands studied. Two systems were prepared. System 1, named 1A2–ANF complex, is 1A2 with bound ANF, while system 2, named 1A2–chrysin complex, is that 1A2 is in complex with chrysin. Same procedures have been subjected to the 2C9/SWF and 2C9/chrysin complexes under identical conditions. As a result, another two systems were prepared. System 3, named 2C9–SWF complex, is 2C9 with bound SWF, while system 4, named 2C9–chrysin complex, is that 2C9 is in complex with chrysin.

MD simulation parameter files were prepared for each system using AMBER 10¹⁸ in this study. Each initial model of four complexes was modeled using Xleap module. The general AMBER force field (GAFF)^{18,19} was used as the parameters for ligands, while AMBER ff03 force field was used as the parameters for 1A2 and 2C9. For the ligands, GAFF parameters were augmented. Based on the

electrostatic potential (ESP) calculations at the ab initio HF/6-31G* level,²⁰ the partial atomic charges of ligands were calculated by using the restricted electrostatic potential (RESP)¹⁹ fitting protocol implemented in the Antechamber module of the AMBER 10 package. The heme cofactor is represented in all simulations with a Cys residue covalently bound to the heme iron and the force field parameters for the heme group were adopted from previously published work.²¹ The four complexes were neutralized by adding sodium counterions, and were solvated in a rectangular box of water molecules with solvent layers 10 \AA between the box edges and solute surface.

Prior to the production step, the following protocol was applied. First, the solutes were fixed, and the solvent molecules with counterions were allowed to move during a 2000 -step minimization. Second, all the atoms were allowed to relax by a 2000 -step full minimization. After the minimization, each complex was gradually heated from 0 to 300 K in 200 ps with solutes constrained at a weak harmonic constraint of $5 \text{ kcal mol}^{-1} \text{ \AA}^{-2}$. Finally, periodic boundary dynamics simulations of 4 ns were carried out with an NPT (constant composition, pressure, and temperature) ensemble at 1 atm and 300 K in the production step. The temperature was kept at 300 K by means of the weak-coupling algorithm.²² The SHAKE algorithm²³ was used to fix all covalent bonds containing hydrogen atoms with a timestep of 2 fs . The Particle-Mesh-Ewald method²⁴ was performed to treat long-range electrostatic interactions. A residue-based cutoff of 10 \AA was utilized for the noncovalent interactions. The output trajectory files were saved every 2 ps for subsequent analysis.

The 500 snapshots isolated from the final 1.0 ns period were employed for the binding free energy calculations by using the MM-PBSA^{25,26} approach encoded in the AMBER 10.0 program. The entropy contribution was not considered because of the similarity of the systems. The detailed information about the binding free energy calculations is provided in Appendix 1.

Our kinetics studies revealed that chrysin selectively bound 1A2. The IC_{50} values of chrysin and ANF towards 1A2 (Fig. 1 and Appendix 2) were 54 nM and 49 nM , respectively. Previously reported IC_{50} values of chrysin and ANF were 200 and 50 nM ,^{27,28} respectively. In addition, the inhibitory affinities of chrysin were determined towards other three isoforms 2C9, 2D6, and 3A4. Our kinetics studies demonstrated that chrysin exhibited relatively weak affinities of 5225 nM , $>50,000 \text{ nM}$, and $>50,000 \text{ nM}$, respectively. Among three isoforms, 2C9 showed about 100 -fold changes on inhibitory sensitivity relative to 1A2. Most dramatic changes were produced by 2D6 and 3A4, which made a loss of at least three orders of magnitudes of sensitivity. The kinetics studies revealed that chrysin achieved higher binding affinity with 1A2 and preferred 1A2 to other three isoforms.

The docking protocol CDOCKER is reliable enough to reproduce the crystal poses of ANF and SWF. In order to achieve the optimal docking configuration and scoring function for two systems (1A2 and 2C9), the ligands ANF and SWF were redocked themselves again into the X-ray structures of 1A2 and 2C9 via a variety of docking conditions and scoring functions, respectively. The root-mean-square deviation (RMSD) values between the optimal docking pose and the crystal one were 0.28 and 0.96 \AA for ANF and SWF (Appendix 3), respectively, which imply that CDOCKER is reliable enough for two systems. Subsequently, chrysin was docked into the same ligand-binding pockets of 1A2 and 2C9 with the same optimal docking parameters and scoring function above.

The MD models can simulate the crystal structures of 1A2 and 2C9. Relative to the X-ray crystal structures, the RMSD values of protein backbone atoms on the 1A2–ANF and 2C9–SWF complexes were monitored (Appendix 4). In both cases, the MD models appeared to reach a stable state after 1 ns equilibration, in which the RMSD values converged below 1.6 \AA . The MD models for the two

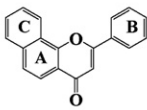
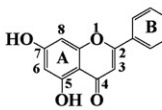
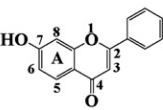
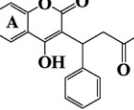
				
	α -naphthoflavone	Chrysin	7-hydroxy-flavone	S-warfarin
Predicted binding free energy (kcal/mol)	-23.54	-23.11/CYP1A2 -20.41/CYP2C9	-20.99	— -27.38
Experimental IC ₅₀ (nM)				
CYP1A2	49	54	240	—
CYP2C9	—	5 225	—	—
CYP2D6	—	>50 000	—	—
CYP3A4	—	>50 000	—	—

Figure 1. The structures, experimental inhibitory affinities (IC₅₀), and predicted binding free energies of α -naphthoflavone, chrysin, 7-hydroxy-flavone, and S-warfarin.

complexes were given in Appendix 5. As shown in Appendix 5, the MD models can simulate the crystal ones of 1A2 and 2C9.

To validate the dynamic stability of the 1A2–chrysin and 2C9–chrysin complexes, the RMSD values along the 4 ns MD trajectories were also monitored relative to the X-ray crystal structures. Appendix 4 gives the RMSD values of the two complexes converged below 1.8 Å, which meant the MD trajectories of the two complexes appeared to be well equilibrated. Therefore, our subsequent analyses in each case were based on the MD trajectories truncated between 3 and 4 ns. The average structures for the 1A2–chrysin and 2C9–chrysin complexes (Fig. 2) were generated by averaging the last 100 snapshots on the MD trajectories. Based on the coordinates of the main C, C α , and N atoms for 481 aligned residues, superposition of the average structure and the X-ray counterpart of 1A2 showed an RMSD value of 1.31 Å, which implied that the average structure exhibited a high similarity in protein backbones and thus verified the accuracy of the simulated average model.

Chrysin bound to 1A2 in a similar pattern as ANF with some exceptions. Hydrophobic/van der Waals' interactions are a crucial element of binding for 1A2. Due to the hydrophobic feature of chrysin, it is reasonable to speculate that the hydrophobic interactions should play an important role in the binding of chrysin to 1A2. The flavone ring of chrysin has common interactions with the 1A2 residues (Fig. 2A). Our structural analysis demonstrated that chrysin bound to the active site of 1A2 in a similar manner as ANF with some exceptions. They stacked against Phe226 and also contacted via hydrophobic/van der Waals' interactions with

residues Thr118, Phe125, Phe260, Gly316, Ala317, Leu497, Thr498, and heme, which held the flavone ring closely in the hydrophobic pocket. The O₁₁ atom of phenolic hydroxyl group formed a H-bond of 2.9 Å with the OD1 atom of Asp313. The O₉ atom was within a hydrogen bonding distance of 2.6 Å to an adjacent water molecule, which also contributed to the binding of chrysin within the active site pocket. In addition, an intermolecular H-bond interaction between the hydroxyl O₁₀ and carbonyl O₉ atoms was maintained along the MD trajectories. They were constricted in a plane with an average distance of 2.6 Å between the two oxygen atoms. The dihedral angle for the four atoms (C₅–O₁₀–O₉–C₄) was monitored along the MD trajectories. As shown in Appendix 6, the angle appeared to reach a stable state from -20° to $+20^\circ$ and thus the molecule exhibited relatively high planarity, which may benefit the van der Waals' interactions between chrysin and the active site. As a result, the energetically favorable van der Waals' and H-bond interactions stabilized chrysin in the active site pocket.

The larger binding site pocket of 2C9 may decrease the van der Waals' interactions with chrysin. For the 2C9–chrysin complex, its averaged structure exhibited a slightly larger RMSD value of 1.71 Å to the X-ray structure and still showed a relatively high similarity in protein backbones. The hydroxyl O₁₀ atom was within hydrogen bonding distance (3.1 Å) of the O atom of Gly98 (Fig. 2B). The O₉ atom formed a weak H-bond with the N atom of Ile99. In addition, a water molecule entered the active site and contributed to the binding of chrysin with 2C9. An H-bond of 3.4 Å was

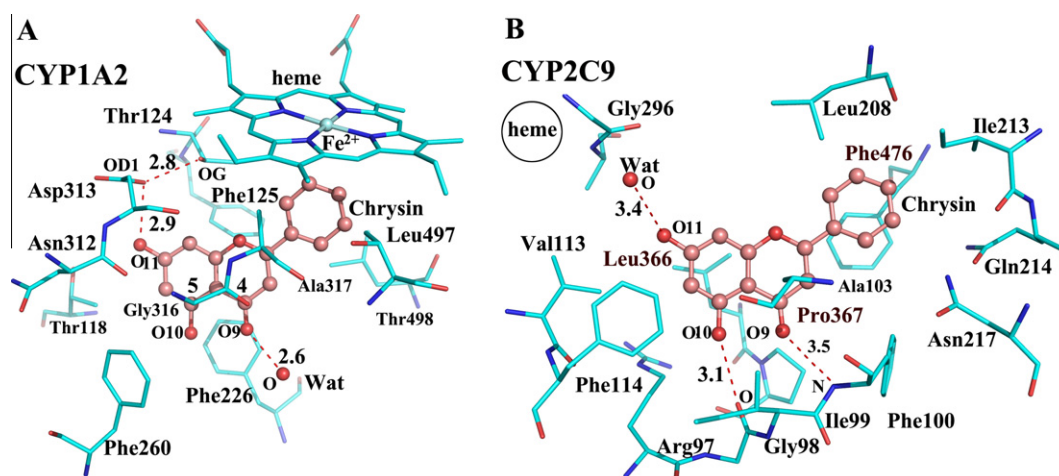


Figure 2. The binding mode of chrysin at the active site of human cytochrome P450 1A2 (A) or 2C9 (B). Chrysin is shown in tint/red colors, while oxygen, carbon, and nitrogen are shown in red, cyan, and blue, respectively. The carbon atoms of five residues (Thr118, Thr124, Phe125, Phe226, and Leu497) behind chrysin (A) are in pale cyan color for clarity relative to other residues. The carbon atoms of three residues (Leu366, Pro367, and Phe476) behind chrysin (B) are in pale cyan color for clarity relative to other residues. A water molecule is represented as a red sphere.

observed between the O atom of the water molecule and the O₁₁ atom of chrysin. Chrysin also contacted with residues Arg97, Phe100, Ala103, Val113, Phe114, Leu208, Ile213, Leu366, Pro367, and Phe476 via van der Waals' interactions. The volume of the active site pocket of 2C9 which is close the heme group was calculated to be 314 Å³ by using the program MOE (Chemical Computing Group Inc., 2008), while that of 1A2 was 202 Å³ after the ligand ANF was removed. The volume of the former is about 50% larger than that of the latter. Thus, the larger and much more open active site architectures of 2C9 (Fig. 3) contrast with the rather compact and closed active site topologies of 1A2 (Appendix 7), which resulted in weaker van der Waals' interactions between 2C9 and chrysin. The weaker van der Waals' interactions may explain the moderate inhibitory affinity of chrysin towards 2C9. The following binding free energy analysis also verified that the van der Waals' interaction energies (ΔE_{vdw}) of the 2C9–chrysin complex were less negative than those of the 1A2–chrysin counterpart.

van der Waals' interactions between chrysin and 1A2 can account for the higher inhibitory affinity. The MM-PBSA method was performed to predict the binding free energies for the four systems. Table 1 lists predicted binding free energies ($\Delta G_{\text{bind, pred}}$) and the decomposition of energy terms, averaged over 500 snapshots for

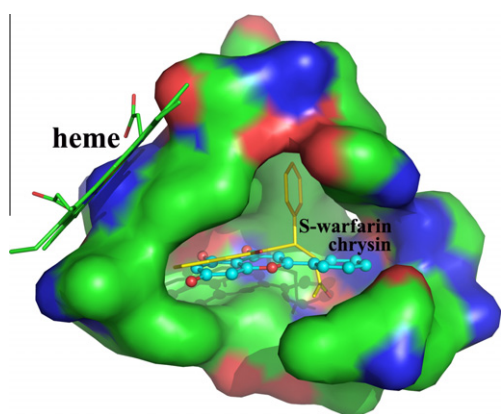


Figure 3. The binding mode of chrysin (CPK, carbon: cyan; oxygen: red) in human cytochrome P450 2C9 after the superposition of the X-ray crystal 2C9 over the MD simulation model in complex with chrysin. The active site pocket which is displayed as a water-accessible surface (probe diameter 1.4 Å) is defined as residues found within 6 Å range of S-warfarin (stick, yellow).

the four simulations. The electrostatic interaction energies ($\Delta E_{\text{ele}} + \Delta G_{\text{ele, sol}}$) for the 1A2–chrysin complex were 5.62 kcal/mol larger than those of the 2C9–chrysin one, but the difference of the van der Waals' interactions (ΔE_{vdw}) were –8.15 kcal/mol for the two complexes. As a result, a more negative value of $\Delta G_{\text{bind, pred}}$ (–23.11 kcal/mol) for the 1A2–chrysin complex than that (–20.41 kcal/mol) for the 2C9–chrysin counterpart, corresponded an enhancement in their binding affinity. The difference in the calculated binding free energies for the two complexes was 2.70 kcal/mol. Consequently, our energetic results revealed that chrysin preferred 1A1 to 2C9, which implied that chrysin exhibited a stronger potency of binding to 1A2 than 2C9. In addition, our energetic analysis demonstrated that van der Waals' and electrostatic/H-bond interactions were the major contributions to the binding of chrysin to 1A2 and 2C9. For the ANF–1A2 complex, the van der Waals interactions were the main driving force for ANF recognition of 1A2.

7-Hydroxyl-flavone bound less strongly to 1A2 than chrysin. Identical computational procedures were applied to 7-hydroxyl-flavone. Based on our docking and MD results, the structural analysis demonstrated that this compound can bind to 1A2 in a similar pattern as chrysin. Its predicted binding free energy was –21.17 kcal/mol (Fig. 1) and slightly less negative than that of chrysin, which corresponded to a decrease in the inhibitory affinity. Compared with chrysin, the absence of the hydroxyl group at the 5th ring position led to a decrease of the architectural planarity and resulted in a reduction of ΔG_{vdw} . The reduction of van der Waals' interactions can explain why 7-hydroxyl-flavone bound less strongly to the enzyme than chrysin.

The relative binding free energies of the two isoforms in complex with chrysin can agree with the experimental measurements. The experimental IC₅₀ values of ANF, chrysin, and 7-hydroxyl-flavone against 1A2 are 49, 54, and 240 nM (Fig. 1), respectively. $\Delta G_{\text{bind, exp}}$ was estimated approximately via $\Delta G \approx RT \ln IC_{50}$ for direct comparison. The $\Delta G_{\text{bind, exp}}$ for the 1A2–chrysin and 2C9–chrysin complexes were –9.95 and –7.25 kcal/mol, while their respective $\Delta G_{\text{bind, pred}}$ were –23.11 and –20.41 kcal/mol, respectively. Since entropic contribution ($T\Delta S$) was excluded, the predicted binding free energies were more negative than those estimated via the experimental IC₅₀ values. However, it is still of significance to compare their relative magnitude, which is common in the literature.^{25,26,29,30} In general, a relative predicted-binding-free energies ($\Delta \Delta G_{\text{bind, pred}}$) of 2.70 kcal/mol refers to about 2.0-fold changes on the experimental inhibitory affinity for chrysin (for example, from 54 nM to 5225 nM) based on the equation. The $\Delta \Delta G_{\text{bind, pred}}$ of

Table 1

Calculated binding free energies and relative energies (kcal/mol) obtained by the Molecular Mechanics Poisson–Boltzmann Surface Area Method

Protein Ligand	CYP 1A2			2C9
	α -Naphthoflavone	Chrysin	7-Hydroxy-flavone	Chrysin
ΔE_{ele}	–0.66 ± 1.65	–11.52 ± 2.86	–10.14 ± 2.67	–13.50 ± 2.03
ΔE_{vdw}	–47.60 ± 1.63	–42.01 ± 2.01	–38.64 ± 2.09	–33.86 ± 1.82
ΔE_{MM}	–47.36 ± 2.24	–53.53 ± 2.49	–48.79 ± 2.42	–47.36 ± 2.59
$\Delta G_{\text{nonpol, sol}}$	–5.07 ± 0.08	–4.58 ± 0.06	–4.56 ± 0.07	–4.41 ± 0.10
$\Delta G_{\text{ele, sol}}$	28.88 ± 2.64	35.01 ± 2.57	32.18 ± 2.50	31.37 ± 2.41
ΔG_{sol}	23.81 ± 2.62	30.42 ± 2.56	27.62 ± 2.48	26.95 ± 2.39
$\Delta G_{\text{bind, pred}}$	–23.54 ± 3.00	–23.11 ± 0.90	–21.17 ± 3.19	–20.41 ± 2.49
$\Delta \Delta G_{\text{bind, pred}}$	–0.43	0.00	1.94	2.70
$\Delta G_{\text{bind, exp}}$	–10.04	–9.95	–9.09	–7.25
$\Delta \Delta G_{\text{bind, exp}}$	–0.09	0.00	0.86	2.70

ΔG_{ele} are electrostatic interactions calculated by the MM force field.

ΔG_{vdw} are van der Waals' contributions from MM.

$\Delta G_{\text{ele, sol}}$ are the polar contribution to solvation.

$\Delta G_{\text{nonpol, sol}}$ are the nonpolar contribution to solvation.

$\Delta G_{\text{MM}} = \Delta G_{\text{ele}} + \Delta G_{\text{vdw}}$ and $\Delta G_{\text{sol}} = \Delta G_{\text{ele}} + \Delta G_{\text{vdw}}$.

$\Delta G_{\text{bind, pred}}$ are predicted binding free energies in the absence of entropic contribution.

$\Delta G_{\text{bind, exp}}$ was estimated approximately via $\Delta G \approx RT \ln IC_{50}$ (Fig. 1).

2.70 kcal/mol between the two complexes agrees with the experimental measurements ($\Delta\Delta G_{\text{bind, exp}} = 2.70$ kcal/mol), which indicates that MD simulations and binding free energy calculations can provide an alternative way to evaluate the isoform selectivity of chrysin. However the theoretical method caused a considerable deviation of 2.49 kcal/mol for the 2C9/chrysin complex, which almost overshadowed the energy difference in the $\Delta G_{\text{bind, pred}}$ for the two complexes. The similar phenomena have been reported in many cases.^{29–32} Though the MM-PBSA method is readily used for a qualitative way to evaluate the inhibitory affinity, one should be cautious in evaluating the $\Delta G_{\text{bind, pred}}$ of the receptor/ligand complexes and better appeal to other methods if an accurate determination of this parameter is needed, especially for some important biological systems for drug discovery purpose.

In addition, the $\Delta G_{\text{bind, exp}}$ of 7-hydroxyl-flavone with 1A2 was -9.09 kcal/mol, which was less negative than that of chrysin. The increasing order in our experimental $\Delta G_{\text{bind, exp}}$ values (chrysin and 7-hydroxyl-flavone) was also consistent with our computational results.

The present study provides a structural insight into the chrysin-bound pattern to 1A2. In the binding mode of chrysin, van der Waals' and electrostatic/H-bond interactions were the driving forces for its recognition of 1A2, while the latter was the primary forces for ANF recognition. The predicted binding free energies for the 1A2–chrysin and 2C9–chrysin complexes were -23.11 and -20.41 kcal/mol, respectively, indicating that the chrysin was more potential for the binding with 1A2. Weaker van de Waal's interactions between 2C9 and chrysin may account for its moderate inhibitory affinity.

The modeling study also revealed that 7-hydroxyl-flavone bound to 1A2 in a similar pattern as chrysin and exhibited a less negative predicted binding free energy, which was validated by our kinetic analysis. Our results indicate that the MD simulations and binding free energy calculations can provide an alternative way to evaluate the inhibitory ability against 1A2 and thus aid the rational molecular design of 1A2 inhibitors with enhanced inhibitory affinities.

Acknowledgments

We thank Dr. Justin Kai-Chi Lau in Department of Chemistry at Hong Kong Baptist University for helpful discussion. The suggestions from the anonymous reviewers are cordially appreciated. We cordially acknowledge the financial support from National Major Projects for Science and Technology Development of China (2009ZX09304-003), Fundamental Research Funds for the Central Universities (10ykjc20), and Natural Science Foundation of Guangdong Province (9451008901001994).

Supplementary data

Supplementary data associated with this article can be found, in the online version, at [doi:10.1016/j.bmcl.2010.08.072](https://doi.org/10.1016/j.bmcl.2010.08.072).

References

- Faber, M. S.; Jetter, A.; Fuhr, U. *Basic Clin. Pharmacol. Toxicol.* **2005**, *97*, 125.
- Butler, M. A.; Iwasaki, M.; Guengerich, F. P.; Kadlubar, F. F. *Proc. Natl. Acad. Sci. U.S.A.* **1989**, *86*, 7696.
- Eaton, D. L.; Gallagher, E. P.; Bammler, T. K.; Kunze, K. L. *Pharmacogenetics* **1995**, *5*, 259.
- Guengerich, F. P.; Parikh, A.; Turesky, R. J.; Josephy, P. D. *Mutat. Res.* **1999**, *428*, 115.
- Murray, G. I.; Shaw, D.; Weaver, R. J.; McKay, J. A.; Ewen, S. W.; Melvin, W. T.; Burke, M. D. *Gut* **1994**, *35*, 599.
- Loe, S. W.; Jang, I. J.; Shin, G.; Lee, K. H.; Yim, D. S.; Kim, S. W.; Oh, S. J.; Lee, S. H. *J. Korean Med. Sci.* **1994**, *9*, 482.
- Birt, D. F.; Hendrich, S.; Wang, W. *Pharmacol. Ther.* **2001**, *90*, 157.
- Moon, Y. J.; Wang, X.; Morris, M. E. *Toxicol. In Vitro* **2006**, *20*, 187.
- Heim, K. E.; Tagliaferro, A. R.; Bobilya, D. J. *J. Nutr. Biochem.* **2002**, *13*, 572.
- Lin, Y. M.; Zhou, Y.; Flavin, M. T.; Zhou, L. M.; Nie, W.; Chen, F. C. *Bioorg. Med. Chem.* **2002**, *10*, 2795.
- Zhou, S.; Gao, Y.; Jiang, W.; Huang, M.; Xu, A.; Paxton, J. W. *Drug Metab. Rev.* **2003**, *35*, 35.
- Kunze, L. K.; William, F. T. *Chem. Res. Toxicol.* **1993**, *6*, 649.
- Cho, U. S.; Park, E. Y.; Dong, M. S.; Park, B. S.; Kim, K.; Kim, K. H. *Biochim. Biophys. Acta* **2003**, *1648*, 195.
- He, F.; Bi, H. C.; Xie, Z. Y.; Zuo, Z.; Li, J. K.; Li, X.; Zhao, L. Z.; Chen, X.; Huang, M. *Rapid Commun. Mass Spectrom.* **2007**, *21*, 635.
- Sansen, S.; Yano, J. K.; Reynald, R. L.; Schoch, G. A.; Griffin, K. J.; Stout, C. D.; Johnson, E. F. *J. Biol. Chem.* **2007**, *282*, 14348.
- Williams, P. A.; Cosme, J.; Ward, A.; Angove, H. C.; Matak, V.; Jhoti, H. *Nature* **2003**, *424*, 464.
- Wu, G.; Robertson, D. H.; Brooks, C. L.; Vieth, M. J. *Comput. Chem.* **2003**, *24*, 1549.
- Case, D. A.; Darden, T. A.; Cheatham, T. E., III, et al. *AMBER 10*; University of California: San Francisco, 2008.
- Wang, J.; Wang, W.; Kollman, P. A.; Case, D. A. *J. Mol. Graph. Model.* **2006**, *25*, 247.
- Frisch, M. J.; Trucks, G. W.; Schlegel, H. B., et al. *GAUSSIAN 03, Revision E.01*; Gaussian: Pittsburgh, PA, 2004.
- Harris, D. L.; Park, J. Y.; Gruenke, L.; Waskell, L. *Proteins* **2004**, *55*, 895.
- Berendsen, H. J. C.; Postma, J. P. M.; van Gunsteren, W. F.; DiNola, A.; Haak, J. R. *J. Chem. Phys.* **1984**, *81*, 3684.
- Miyamoto, S.; Kollman, P. A. *J. Comput. Chem.* **1992**, *13*, 8952.
- Darden, T.; York, D.; Pedersen, L. J. *J. Chem. Phys.* **1993**, *98*, 10089.
- Fogolari, F.; Brigo, A.; Molinari, H. *Biophys. J.* **2003**, *85*, 159.
- Kollman, P. A.; Massova, I.; Reyes, C., et al. *Acc. Chem. Res.* **2000**, *33*, 889.
- Weaver, R.; Graham, K. S.; Beattie, I. G.; Riley, R. J. *Drug Metab. Dispos.* **2003**, *31*, 955.
- Iori, F.; da Fonseca, R.; Joao Ramosb, M.; Menziania, M. C. *Bioorg. Med. Chem.* **2005**, *13*, 4366.
- Liu, M.; Yuan, M.; Luo, M.; Bu, X.; Luo, H.-B.; Hu, X. *Biophys. Chem.* **2010**, *147*, 28.
- Neugebauer, R. C.; Uchietowska, U.; Meier, R., et al. *J. Med. Chem.* **2008**, *51*, 1203.
- Zeng, J.; Li, W. H.; Zhao, Y. X.; Liu, G. X.; Tang, Y.; Jiang, H. L. *J. Phys. Chem. B* **2008**, *112*, 2719.
- Luo, H.-B.; Zheng, H.; Zimmerman, M. D.; Chruszcz, M.; Skarina, T.; Egorova, O.; Savchenko, A.; Edwards, A. M.; Minor, W. J. *Struct. Biol.* **2010**, *169*, 304.